Electronic Properties of $ZnPSe_3$-MoS_2 Van der Waals Heterostructure

Munish Sharma[1, a)], Ashok Kumar[2] and P. K. Ahluwalia[1]

[1]*Department. of Physics, Himachal Pradesh University, Shimla, H. P., 171005 (India)*
[2]*Centre for Physical Science, School of Basic and Applied Sciences, Central University of Punjab, Bathinda, 151001 (India)*
[a)]*Corresponding author: munishsharmahpu@live.com*

Abstract. We present a comparative study of electronic properties of $ZnPSe_3$-MoS_2 heterostructure using GGA-PBE functional and DFT-D2 method within the framework of density functional theory (DFT). Electronic band structure for the considered heterostructure shows a direct band gap semiconducting character. A decrease in band gap is observed with the heterostructuring as compared to their constituent pristine monolayers. The alignment of valance band maxima and conduction band minima on different layers in heterostructure indicate the physical separation of charge carriers. A work function of 5.31 eV has been calculated for $ZnPSe_3$-MoS_2 heterostructure. These results provide a physical basis for the potential applications of these $ZnPSe_3$-MoS_2 heterostructure in optoelectronic devices.

INTRODUCTION

Layered transition metal dichalcogenides (TMDs) among the family of two dimensional (2D) materials beyond graphene have shown potential to fulfill the demands of current nano-electronics industry. There is a rapid pace of progress on the studies of van der Waal's heterostructure consisting of two different 2D materials in last few years [3-5]. Very recently, atomically thin layers of metal phosphorous Trichalcogenides have been synthesized experimentally offering a wide range of band gap [1-2]. The layer by layer arrangement of these two dimensional materials offers an interesting way to build heterostructure multilayers in controlled manner. In this work we present a comparative study of electronic properties of $ZnPSe_3$-MoS_2 Van der Waal heterostructure (figure 1) using GGA-PBE and DFT-D2 method vis-à-vis their pristine structures.

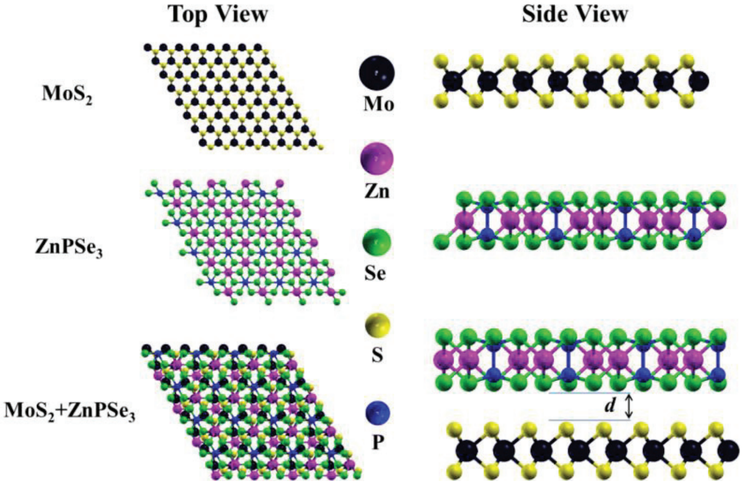

;

FIGURE 1. Ball and stick model with respective top and side view for pristine MoS_2, $ZnPSe_3$ and their heterostructures (MoS_2+$ZnPSe_3$).

DAE Solid State Physics Symposium 2017
AIP Conf. Proc. 1942, 120019-1–120019-4; https://doi.org/10.1063/1.5029059
Published by AIP Publishing. 978-0-7354-1634-5/$30.00

SIMULATION DETAILS

The calculations have been performed by using Vienna *ab initio* simulation package (VASP) [6] based on density functional theory (DFT). An ion-electron interaction has been taken care with the projector-augmented plane wave (PAW) method. A GGA-PBE functional has been used to describe the exchange correlation term. The van der Waals interactions resulting from dynamical correlations between fluctuating charge distribution was described within the DFT-D2 method of Grimme [7]. To minimize the interaction between the periodic images a vacuum of about 15 Å along c axis has been introduced. A kinetic-energy cutoff of 400 eV is used. Structure has been fully relaxed until the force on each atom is less than 0.01 eV/Å. Monkhorst-Pack grid of 15x15x1 have been used to sample the brillouin-zone. The energy convergence criteria of 10^{-6} eV has been used in self-consistent electronic steps.

RESULTS AND DISCUSSION

Our calculations begin with the full relaxation of pristine MoS_2 and $ZnPSe_3$. We find an optimized lattice constant of 3.19 and 6.29 Å for MoS_2 and $ZnPSe_3$ respectively. Our calculated values are in very good agreement with the previously reported values [8-10]. For the $ZnPSe_3$-MoS_2 heterostructure, a supercell of 2x2x1 for MoS_2 and pristine unit cell for $ZnPSe_3$ result a tensile strain of +1.41 % in $ZnPSe_3$. The minimization of total energy results in optimized vertical interlayer separation of 3.95 and 3.47 Å for $ZnPSe_3$-MoS_2 heterostructure with GGA-PBE functional and DFT-D2 method respectively (table 1). To ensure the stability of the $ZnPSe_3$-MoS_2 heterostructure, we have calculated the binding energy (E_b) as

$$E_b = E_{ZnPSe_3-MoS_2} - (E_{ZnPSe_3} + E_{MoS_2}) \qquad (1)$$

Where $E_{ZnPSe_3-MoS_2}$ is total energy of $ZnPSe_3$-MoS_2 heterostructure, E_{MoS_3} and E_{ZnPSe_3} are the total energy of MoS_2 and $ZnPSe_3$ monolayer units, respectively, obtained from converged VASP runs. The binding energy is found to be -0.29 and -0.72 eV with GGA-PBE and DFT-D2 method respectively (table 1). The stronger binding found with the DFT-D2 method is attributed to smaller interlayer separation in this case as compared to GGA-PBE functional. The negative adsorption energies indicate the exothermic process.

Electronic Properties

MoS_2 monolayer a semiconductor having a direct band gap of 1.60 eV [8-10]. The electronic band structures of pristine $ZnPSe_3$ and its heterostructure with MoS_2 has been calculated along high symmetry Γ-M-K-Γ directions. Figure 2 shows the atom projected electronic band structure and corresponding density of states for pristine $ZnPSe_3$ and its heterostructure with MoS_2. The pristine $ZnPSe_3$ is an indirect band gap semiconductor with valance band maxima at 'K' and conduction band minima at 'Γ'. The calculated band gap of monolayer $ZnPSe_3$ is 1.32 eV with GGA-PBE functional and DFT-D2 method. These results are consistent with the previous reports [2].

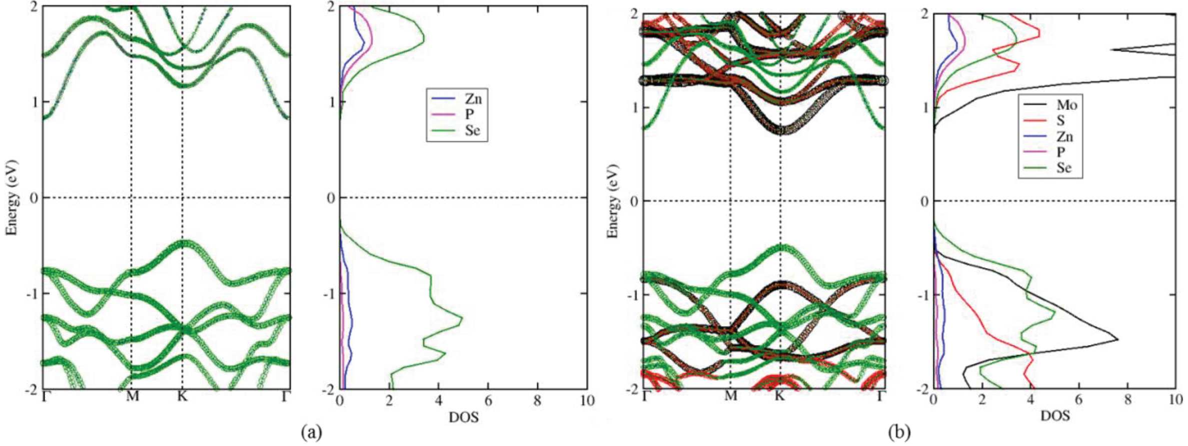

(a) (b)

FIGURE 2. Band structure and corresponding atom projected density of states for pristine $ZnPSe_3$ and MoS_2+$ZnPSe_3$. The colors of the bands and DOS have same color scheme. Widths of the bands show the weight factor.

It is clear from the figure 2(b) that the $ZnPSe_3$-MoS_2 heterostructure exhibits a direct band gap with VBM and CBM at 'K' point. A direct band gap of 0.99 eV and an indirect band gap of 1.02 eV have been observed for $ZnPSe_3$-MoS_2 heterostructure with DFT-D2 method. Note that the DFT-D2 method estimates ~100 meV lower values of band gap as compared to that obtained with GGA-PBE functional (table 1). This lowering in band gap can be attributed to the different equilibrium interlayer separation (d) with GGA-PBE functional and DFT-D2 method. The density of state analysis suggests that contribution to VBM originates from Se atom and CBM from Mo atoms. This indicates that VBM and CBM are localized on different layers suggesting the physical separation of charge carriers.

TABLE 1. Interlayer sepration (d), binding energy (E_b), band gap (E_g) and work function (Φ) for $ZnPSe_3$+MoS_2 heterostructure.

System	d (Å)		E_b (eV)		E_g (eV)		Φ (eV)	
	DFT-D2	GGA-PBE	DFT-D2	GGA-PBE	DFT-D2	GGA-PBE	DFT-D2	GGA-PBE
$ZnPSe_3$ +MoS_2	3.47	3.95	-0.72	-0.29	0.99	0.89	5.12	5.10

To understand the change in electronic band structure we have also carried out charge density analysis. Figure 3 depicts the charge density at VBM, at CBM and charge density difference. The charge density difference has been calculated as difference between the total charge density of composite system ($\rho_{ZnPSe_3-MoS_2}$) and sum of isolated charge density of $ZnPSe_3$ and MoS_2 (ρ_{MoS_3} , ρ_{ZnPSe_3}) i.e.

$$\Delta\rho = \rho_{ZnPSe_3-MoS_2} - (\rho_{ZnPSe_3} + \rho_{MoS_2}) \qquad (2)$$

The red and green regions show positive and negative charge, respectively. The red color on the Se atom in case of VBM charge density and on Mo atom in case of CBM confirms that the charge carriers are physical separated as they are localized on different layers. Charge density difference profile indicates a significant charge redistribution which essentially causes reduction in effective band gap.

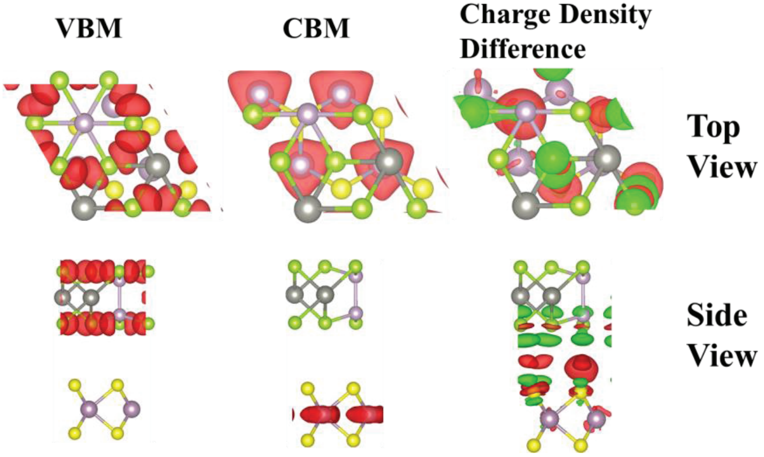

FIGURE 3. Top and side view of charge density at VBM, CBM and charge density difference profile for MoS_2+$ZnPSe_3$ heterostructure.

Furthermore, there are certain physical phenomena such as thermionic emission, band offsets, and contact current which are highly sensitive to the work function of the material. Therefore, we have also calculated work function for the pristine $ZnPSe_3$, MoS_2 and their heterostructure. The work function (Φ) of the 2D materials before and after making heterostructure have been calculated using following equation

$$\Phi = E_{Vac} - E_f \qquad (3)$$

where E_{Vac} and E_f are the electrostatic potential at the vacuum level and Fermi energy, respectively. We find a work function of 5.36 eV for $ZnPSe_3$. The work function for monolayer MoS_2 is 5.51 eV which is in good agreements with the experimentally measured value of 5.25 eV [11]. The heterostructuring has lead to reduction in work function to the 5.10 eV. Note that the calculated work function does not depend upon the type of method used (GGA-PBE functional or DFT-D2 method) for the studied case.

CONCLUSIONS

In conclusion, we have performed a comparative first principle calculations to study the electronic properties of $ZnPSe_3$-MoS_2 heterostructure with GGA-PBE functional and DFT-D2 method. We find a strong binding of -0.72 eV and -0.29 eV with GGA-PBE functional and DFT-D2 method, respectively which is attributed to the different optimized interlayer separation for both the cases. The band gap of 0.89 and 0.99 eV has been found in $ZnPSe_3$-MoS_2 heterostructure with GGA-PBE functional and DFT-D2 method respectively. The work function of 5.36, 5.51 and 5.10 has been calculated for $ZnPSe_3$, MoS_2 monolayer and $ZnPSe_3$-MoS_2 heterostructure respectively. Our study reveals that it is worth investigating other heterostructure from the family of metal phosphorous trichalcogenide with MoS_2 for new insights and technological applications.

ACKNOWLEDGMENTS

Munish Sharma wishes to acknowledge the DST, govt. of India, New Delhi for providing the financial support in the form of INSPIRE Fellowship. CVRAMAN, high performance computing cluster at Himachal Pradesh University has been used to obtain the results presented in this paper.

REFERENCES

1. K. Du, X. Wang et. al. ACS Nano **10,** 1738-1743 (2016).
2. J. Liu, X. Li et. al. Journal of Chemical Physics **140**, 054707 (2014)
3. C. Li, Peng Zhou and David Wei Zhang, Journal of Semiconductors **38(3)** (2017)
4. Z. Lin, A. McCreary et. al. 2D Mateials. **3** 042001 (2016)
5. M Sharma, P Jamdagni, A Kumar, PK Ahluwalia, Physica E: Low-dimensional Systems and Nanostructures **71**, 49-55 (2015)
6. G. Kresse and D. Joubert, Phys. Rev. B, **59**, 1758-1775 (1999)
7. J. Harl, L. Schimka, and G. Kresse, Phys. Rev. B **81**, 115126 (2010).
8. Y. Wang, B. Wang, R. Huang, B. Gao, F. Kong and Q. Zhang, Phys. E, **63**, 276-282 (2014).
9. K. F. Mak, C. Lee, J. Hone, J. Shan and T. F. Heinz, Phys. Rev. Lett., **105**, 136805 (2010)
10. M Sharma, GC Loh, G Wang, R Pandey, SP Karna, PK Ahluwalia RSC Advances **6 (45)**, 38499-38504 (2016)
11. J. H. Kim, J. Lee et. al. Appl. Phys. Lett. , **103**, 033122 (2013)